

Magnetoresistance in microwave synthesized $\text{Ag}_{2+\delta}\text{Se}$ ($0.0 \leq \delta \leq 0.2$)

S. Sundar Manoharan* and S. John Prasanna

Materials Chemistry Lab, Department of Chemistry, Indian Institute of Technology, Kanpur-208016, India

D. Elefant Kiwitz and C. M. Schneider

Institute for Solid State Research, 20 Helmholtz Strasse, D-01069 Dresden, Germany

(Received 8 January 2001; published 11 May 2001)

Compositional variation of magnetoresistance (MR) ratio with silver excess stoichiometry in $\text{Ag}_{2+\delta}\text{Se}$ samples has been studied employing a synthetic approach to prepare instantly a series of bulk silver selenide compounds using microwave energy. Bulk density $>99\%$ is achieved *in situ*, by means of volumetric heating/sintering in less than 10 min, which makes this process unique compared to other chemical and nonchemical approaches. We observe a systematic decrease in metal-insulator transition with increasing Ag. Magnetoresistance ratio observed in transverse geometry is 145%, greater than the longitudinal geometry (70%). This series shows linear dependence of MR with higher fields ($3 < H < 16$ T) with no saturation of MR ratio even at 16 T in transverse mode. However, a distinct saturation effect was noticed in almost all the compositions for magnetic field above 13 T in longitudinal mode. Electron probe microanalysis shows an elemental-rich selenium phase for $\delta=0.05$ composition which accounts for low resistivity, large magnetoresistance ratio and unsymmetrical MR curves when field is applied in both the directions. This is attributed to the charge density fluctuations in chemically inhomogeneous systems. At 300 K, MR ratios of 30 and 59 % for $\delta=0.2$, in longitudinal and transverse mode is observed, respectively.

DOI: 10.1103/PhysRevB.63.212405

PACS number(s): 75.80.+q, 72.80.Jc, 72.90.+y

Silver chalcogenides $\text{Ag}_{2+\delta}\text{Se}$, $\text{Ag}_{2+\delta}\text{Te}$, are distinguished as the only nonmagnetic and nonstoichiometric class of compounds¹ to show unique magnetoresistive (MR) properties. They are narrow gap, self-doped, and degenerate *n*-type semiconductors, showing positive magnetoresistance ratio $\Delta\rho/\rho_0$ up to 370% at $T=4.5$ K and $B=5.5$ T.²⁻³ This origin of MR stems from the orbital magnetoresistance which is related to the ratio of cyclotron frequency to the scattering rate $\omega_c\tau \sim eH\tau/m^*c$. For $\omega_c\tau > 1$, low carrier density semiconductors are expected to show positive MR, quadratic at low field and saturating at high field. With vanishing Hall effect, non-saturating response even at high magnetic fields is expected, which is the case with the Ag_2Se and Ag_2Te films reported so far.⁴⁻⁵ Unlike other magnetoresistive materials, the origin of MR in silver chalcogenides is discussed and tentatively assigned to its complex structure. Key variable in the optimization of the magnetoresistance is (i) the electron density and Hall mobility, μ which depends on the electronic and point defects, (ii) the microstructure, and (iii) the texture of the thin films. In otherwise relatively well-studied $\text{Ag}_{2+\delta}\text{Te}$ films, unusual positive MR and negative MR are observed simultaneously when magnetic field is applied along two opposite directions, perpendicular to the film surface. Such unusual MR behavior is correlated to the textured growth, doping concentration and to the annealing time.⁴ Also textured films seemingly exhibit pronounced MR ratio compared to the bulk samples.⁵ Hitherto no correlations have been made between the microstructure and compositional changes to the high field, nonsaturating MR behavior. In this paper, first we describe a one-step rapid synthetic route to prepare and sinter (*in situ*), $\text{Ag}_{2+\delta}\text{Se}$ samples using microwave radiation.^{6,7} This process enables us to achieve well sintered, oriented samples with density $>99\%$ of the theoretical value. Secondly, we show possible correlation be-

tween the microstructure and the resistivity dependence and thirdly we demonstrate that at high fields $H > 13$ T, saturation of MR is possible in the longitudinal mode.

Bulk sintered $\text{Ag}_{2+\delta}\text{Se}$ samples were prepared employing a commercial microwave oven with 900 W, and 2.45 GHz frequency. Stoichiometric amounts of spectroscopic grade Ag (99.9%) and Se (99.9%) purity intimately mixed and compacted into cylindrical rods of 10 mm \times 3 mm dimension and was evacuated in a quartz tube. The sealed quartz ampules were exposed to microwave radiation at high power level for up to 10 min. During the exposure bright flashes were observed due to excitation and de-excitation of elemental Se. As a result an *in situ* exothermic reaction occurs which instantly leads to product formation. Further, due to volumetric heating throughout the sample, *in situ* sintering occurs simultaneously. This process distinguishes itself as a unique approach compared to other chemical routes.

The samples were tested for powder x-ray diffraction using crushed samples. Cylindrical rods of dimension 2 mm \times 8 mm were polished and employed for four probe resistivity measurements. Magnetoresistive measurements were made employing a 16 T magnet. Polished samples were used for studying the surface morphology. Electron probe microanalysis (employing JXA 8600 MX model) was performed for Ag and Se mapping and also to study the relative composition of Ag and Se in each samples.

Figure 1 shows the powder x-ray patterns for the Ag excess compositions. All the samples crystallize in orthorhombic symmetry. There is an overall lattice contraction with increase in excess silver doping. The peak broadening indicates the fine particulate nature of the powdered crystallites obtained from the cylindrical rods. No significant correlation could be drawn from the intensity of the reflections corresponding to (013) and (004) reflections as discussed for the

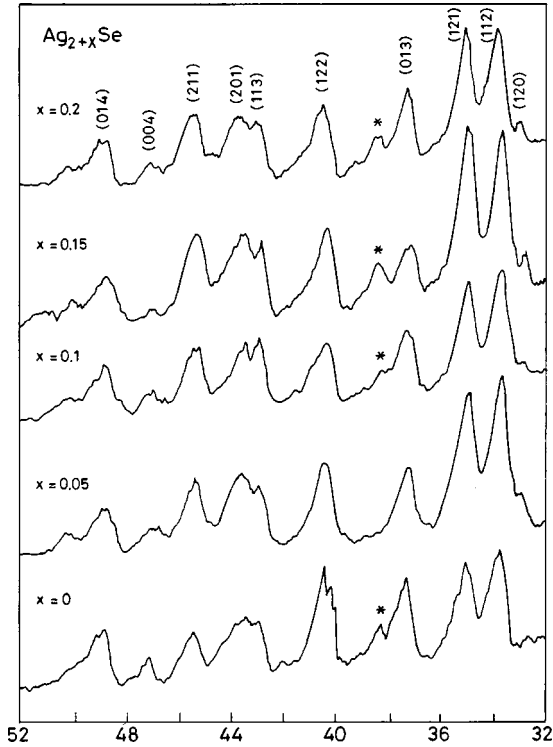


FIG. 1. The plot of the powder x-ray-diffraction pattern of the microwave synthesized $\text{Ag}_{2+\delta}\text{Se}$ polycrystalline samples ($0 < \delta \leq 0.2$). All samples crystallize in orthorhombic symmetry. With excess silver, an overall decrease in cell volume is noted. A silver excess Ag(111) peak is observed (asterisk) for $0 < \delta \leq 0.2$.

observation of n -MR and p -MR in textured $\text{Ag}_{2+\delta}\text{Te}$ samples.⁴ With increase in Ag doping a small peak corresponding to silver (111) was observed in all the samples.

In Fig. 2, we show the plot of normalized resistance versus temperature. A typical small band gap behavior was noted with resistance gradually increasing with decreasing temperature. At a critical temperature T_{crit} the resistance value reaches a maximum and then on, it decreases due to progressive decrease in phonon scattering process. The temperature dependence of resistance is consistent with the impurity band electron on the delocalized side of the Mott-insulator transition. A significant temperature independent resistivity behavior was noted (inset to Fig. 2) for all samples below 20 K. The T_{crit} at which the maximum of resistivity is observed, varies from 105–130 K for $0.0 < \delta < 0.2$. These values are higher than those reported by Xu *et al.*² but lower enough than the values reported by Ogarelec *et al.*³ While a monotonic change in T_{crit} is noted up to $\delta \sim 0.2$, there is a significant increase in resistivity for the Ag excess compositions.

Figures 3(a)–3(c) shows the SEM micrograph of $\delta = 0.0$, 0.05, and 0.2 compositions. It is noteworthy that the SEM microscopic studies reveal that all the compositions show excellent oriented grains with a distinct sintered density of $>99\%$. Except for $\delta = 0.05$, all the samples showed grains oriented along one direction. However $\delta = 0.05$ shows a disoriented feature. On carefully analyzing the intensity ratios of $I_{\text{Ag}(2.98 \text{ eV})}/I_{\text{Se}(11.22 \text{ eV})}$ (see Fig. 4(a)) we observe a distinct

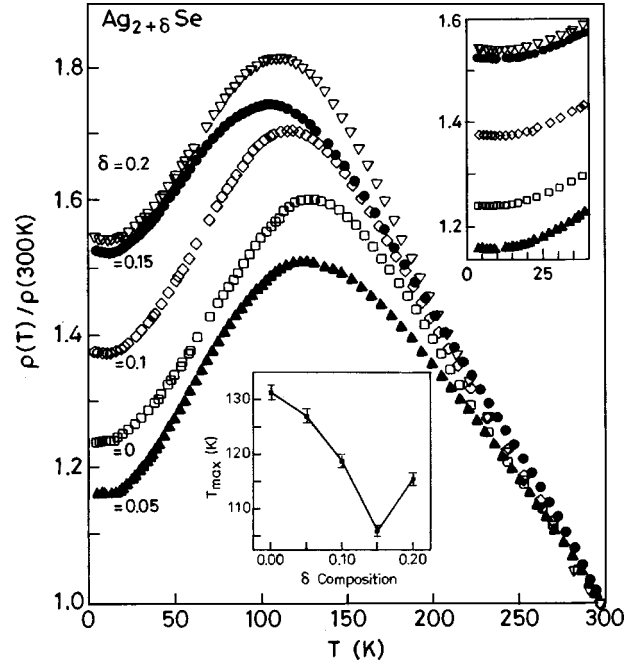
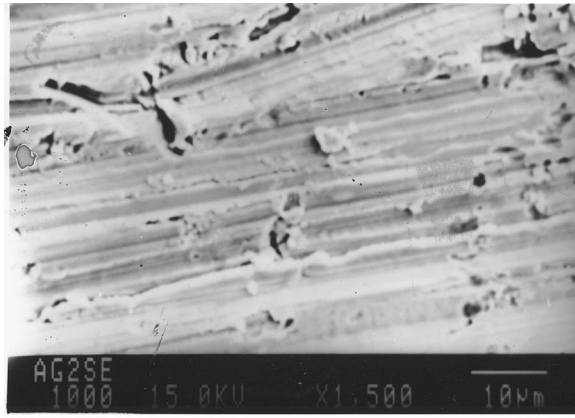


FIG. 2. The plot of normalized resistance versus temperature for $\text{Ag}_{2+\delta}\text{Se}$ bulk samples. Note the monotonic shift in T_{crit} with increasing Ag content. The inset shows the T_{crit} dependence on the silver excess composition.

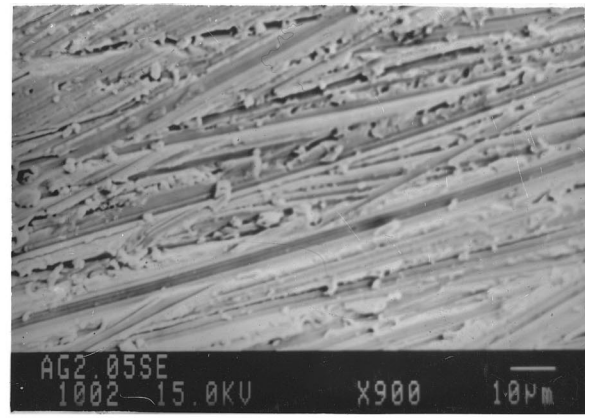
decrease in the ratio for $\delta = 0.05$ indicating that there is a Se-rich surface unlike other compositions. Such Se-rich surface seemingly modifies the resistivity behavior (to higher conductivity as seen in Fig. 2). This implies that at low carrier density concentrations, density fluctuations can greatly influence the conduction electrons. This nonmonotonic behavior of normalized resistance for $\delta = 0.05$ composition is further reflected in the MR data with $B \perp I$ for $T < T_{\text{crit}}$.

Shown in Fig. 4(b) is the plot of MR ratio versus Ag excess composition. For $\delta = 0.05$ an overall decrease in resistance leads to increased magnetoresistance. At 4.2 and 115 K an MR ratio of 145 and 98% is observed for $T < T_{\text{crit}}$, which is higher than all other compositions. Such a pronounced behavior also leads to unsymmetrical MR curve for $\delta = 0.05$ [Fig. 5(a)] when the field is applied along both $B \perp I$ direction, unlike other compositions. Although earlier studies^{4,5} show that unsymmetrical nature of the MR curve is correlated to texture and preferred orientation of the film, we observe that its due to compositional variation in the sample. Se-rich sample, hence modifies both the resistivity behavior and the MR characteristics.

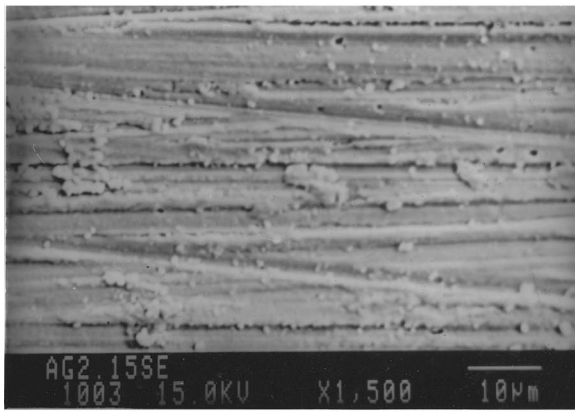
Except for this apparent difference for $\delta = 0.05$ sample, there are nevertheless some common features. All the samples measured at 4.2 K show a quadratic field dependence of the magnetoresistance $\Delta\rho/\rho_0 = K\mu_d^2 B^2$ at lower fields and $\Delta\rho/\rho_0 = \alpha(B - B_0)$ at higher fields. For samples measured at room-temperature, the quadratic dependence extends up to around 3 T, with $B \perp I$ and $B \parallel I$. MR in longitudinal mode shows a reverse but systematic trend in MR ratio as a function of Ag doping. The values are higher for low carrier density concentration 70% for $\delta = 0.0$, 62% for δ



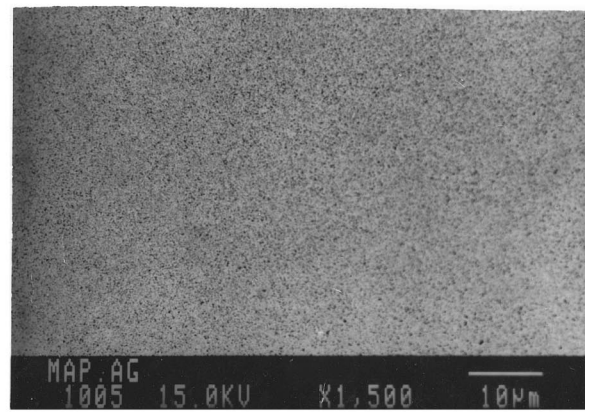
(a)



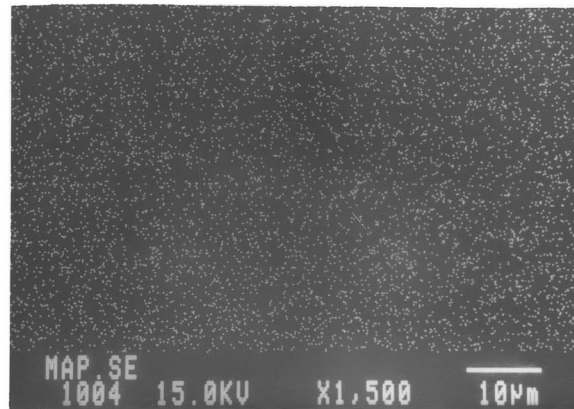
(b)



(c)



(d)



(e)

FIG. 3. (a)–(c) The electron probe microanalysis picture of the surfaces of Ag_2Se , $\text{Ag}_{2.05}\text{Se}$, and $\text{Ag}_{2.15}\text{Se}$ samples prepared by the microwave method wherein *in situ* sintering occurs simultaneously. Note the unusual misorientation of grains for the $\delta=0.05$ composition for which the EPMA analysis of $I_{\text{Ag}(2.98\text{eV})}/I_{\text{Se}(11.22\text{eV})}$ ratio suggests a Ag-lean surface. (d) and (e) The EPMA mapping of silver and selenium $\delta=0.0$ composition showing uniform distribution of both the elements.

$=0.1$, and 57% for $\delta=0.2$. However noteworthy of all is the significant field saturation which is observed for 0.2 composition at 13 T. This is in accordance with the behavior expected in metals, where, saturation at high and low fields are

expected in $B \perp I$ and $B \parallel I$, respectively.⁸

In summary, we observe that compositional inhomogeneity leads to anomalous resistivity behavior, unsymmetrical MR curves and higher MR values in transverse geometry.

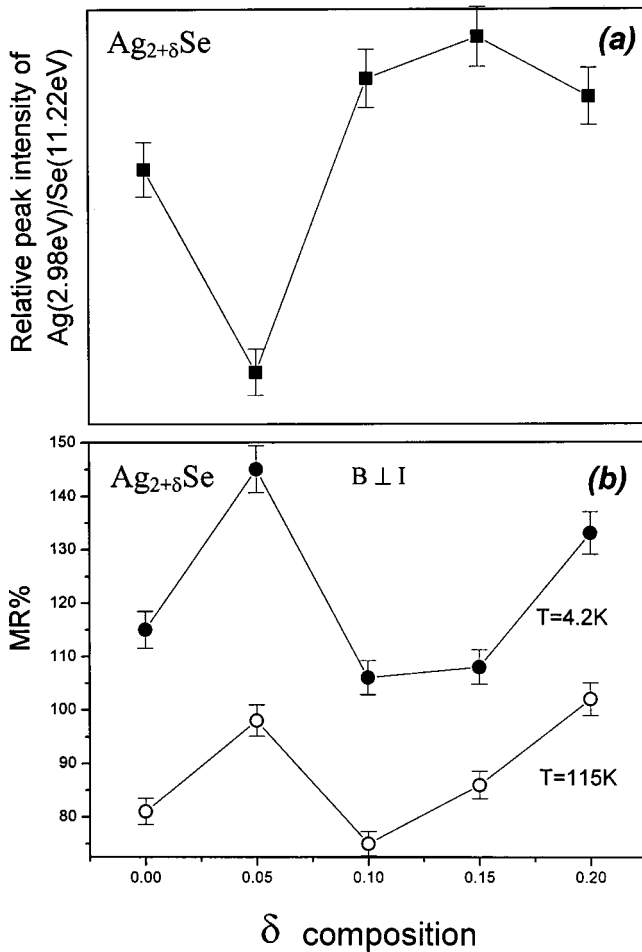


FIG. 4. (a) The peak intensity ratio of $I_{\text{Ag}(2.98\text{eV})}/I_{\text{Se}(11.22\text{eV})}$. It clearly indicates that there is a depletion of silver concentration from the calculated stoichiometric amount. (b) The MR ratio versus composition at 4.2 and 115 K. Note the inverse dependence of the peak intensity ratio with MR ratio for $\delta=0.05$ composition.

This is attributed to the carrier density fluctuations. Field saturation of MR is observed for higher silver excess compositions. We also observe that the microwave process holds promise for preparing chalcogenides instantly.

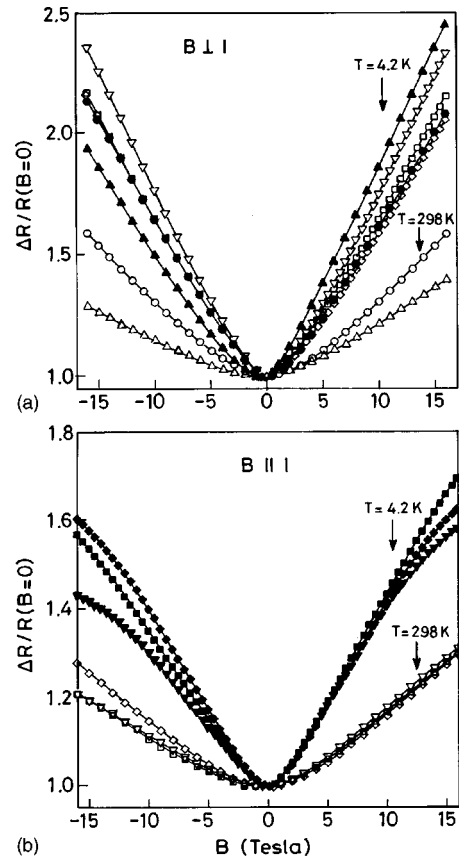


FIG. 5. (a) The MR ratio versus field, applied perpendicular to the current (where $\square = \text{Ag}_2\text{Se}$, $\blacktriangle = \text{Ag}_{2.05}\text{Se}$, $\diamond = \text{Ag}_{2.1}\text{Se}$, $\bullet = \text{Ag}_{2.15}\text{Se}$, $\nabla = \text{Ag}_{2.2}\text{Se}$ at 4.2 K). The unsymmetrical nature of the curve is noted in $\text{Ag}_{2.05}\text{Se}$ composition. At 298 K $\circ = \text{Ag}_{2.15}\text{Se}$ (52%) and $\triangle = \text{Ag}_{2.05}\text{Se}$ (40%) is noted. (b) The MR versus applied field parallel to the current direction at 4.2 K ($\blacksquare = \text{Ag}_2\text{Se}$, $\blacklozenge = \text{Ag}_{2.1}\text{Se}$, and $\blacktriangledown = \text{Ag}_{2.2}\text{Se}$) and at 298 K (where $\square \approx \text{Ag}_2\text{Se}$, $\diamond = \text{Ag}_{2.1}\text{Se}$, $\nabla = \text{Ag}_{2.2}\text{Se}$). Note the field saturation of MR at 16T for $\nabla = \text{Ag}_{2.2}\text{Se}$ at 4.2 K.

CSIR Grant No. EMR(II)-1515 is greatly acknowledged. We thank Mr. R. P. Singh for his kind help in EPMA studies. S.S.M. thanks IFW for financial support. We thank Professor A. K. Nigam (TIFR) for verifying our resistivity data.

*Author to whom correspondence should be addressed. Email address: ssundar@iitk.ac.in

¹P. Junod, H. Hediger, B. Kilchor, and J. Wullschlegler, *Philos. Mag.* **36**, 941 (1977).

²R. Xu, A. Husmann, T. F. Rosenbaum, M. L. Saboungi, E. J. Enderby, and P. B. Littlewood, *Nature (London)* **390**, 57 (1997).

³Z. Ogorelec, A. Hamzic, and M. Basletic, *Europhys. Lett.* **46**, 56 (1999).

⁴B. Q. Liang, X. Chan, Y. J. Wang, and Y. J. Tang, *Phys. Rev. B*

61, 3239 (2000).

⁵I. S. Chuprakov and K. H. Dahmen, *Appl. Phys. Lett.* **72**, 2165 (1998).

⁶C. C. Landry and A. R. Barron, *Science* **260**, 1653 (1993).

⁷A. G. Whittaker and D. M. P. Mingos, *J. Chem. Soc. Dalton Trans.* **1992**, 2751.

⁸W. Jones and N. H. March, *Non-Equilibrium and Disorder*, Vol. 2 of *Theoretical Solid State Physics* (Wiley Ltd., London, 1973).